Miniaturized CPW-Fed Planar Monopole Antenna for Multi-band WLAN/WiMAX Wireless Applications

Ahmed Zakaria Manouare[1], Divitha Seetharamdoo[2], Saida Ibnyaich[3], Abdelaziz El Idrissi[1], Abdelilah Ghammaz[1]

[1] *Department of Applied Physics, Laboratory of Electrical Systems and Telecommunications, Faculty of Sciences and Technologies, Cadi Ayyad University, 40000 Marrakesh, Morocco*
[2] *Univ. Lille Nord de France, The French Institute of Science and Technology for Transport, Development and Networks (IFSTTAR), LEOST Laboratory, 59650 Villeneuve d'Ascq, France*
[3] *I2SP Research Team, Faculty of Sciences Semlalia, Cadi Ayyad University, 40000 Marrakesh, Morocco*

To incorporate two different communication standards in a single device, a miniaturized dual-band planar monopole antenna is presented in this paper. The proposed antenna is formed by a CPW feed line and a rectangular ring monopole with a vertical strip. The designed antenna has a small overall size of 19 mm × 36 mm × 1.6 mm. A prototype of the proposed antenna which was fabricated and measured to validate the design shows a good agreement between the simulation and the experiment. The measured results indicate that the antenna has the impedance bandwidths of 650 MHz (2.30-2.95 GHz) and 2460 MHz (3.40-5.86 GHz) at the first and second bands, respectively with a reflection coefficient less than − 10 dB covering all the WLAN bands (2.4/5.2/5.8 GHz) and WiMAX bands (2.6/3.5/5.5 GHz). In addition, the nearly omni-directional and bi-directional radiation patterns are also achieved in both H- and E-planes, respectively. It is also noticeable that a good antenna gain over both operating bands has been obtained. Therefore, this simple compact planar monopole antenna with multi-band characteristics is well suitable for WLAN and WiMAX wireless communication applications. Details of the proposed antenna design and both simulated and experimental results are analyzed and discussed.

Keywords: Coplanar waveguide (CPW) feed, Miniaturized antenna, Planar monopole antenna, Multi-band characteristics, WLAN/WiMAX wireless applications.

1. INTRODUCTION

In the last decades, there has been a rapid progress in wireless communications technology employing various frequency bands. It is advantageous for a single wireless system to have an access to several services in which two or more bands with acceptable separation are required. Normally a dual-band or multi-band antenna is required to fit in many services in one device such as Wireless Local Area Network (WLAN) and Worldwide Interoperability for Microwave Access (Wi-MAX) as these two technologies are now amply used in wireless communication devices. To satisfy the IEEE 802.11 WLAN bands in the 2.4/5.2/5.8 GHz (2.4–2.484 GHz/ 5.15–5.35 GHz/ 5.725–5.825 GHz) and WiMAX bands in the 2.6/3.5/5.5 GHz (2.5–2.69 GHz/ 3.4–3.69 GHz/ 5.25–5.85 GHz), the multi-band planar antennas with low profile and weight, low cost, compact size, ease of integration with other circuits and higher performance are certainly required to cover all these operating bands for different standards.

Dual-band and multi-band antennas for communication applications are especially attractive. They not only take the task of multi-band working, but also eliminate the need of two or more separate antennas, thus avoiding the isolation problem existing between several antennas. Various studies of multi-band antennas designed for WLAN (2.4/5.2/5.8 GHz) and WiMAX (2.6/3.5/5.5 GHz) applications have been reported in [1-8]. A microstrip slot triple-band antenna and a CPW-fed monopole antenna with double rectangular rings and vertical slots in the ground plane are presented in

[1, 2]. In [3, 4], an inverted L-slot antenna with defected ground structure and a square-slot antenna with symmetrical L-strips are proposed. A printed antenna with three circular-arc-shaped strips and a circular ring antenna with a Y- shape-like strip and a defected ground plane are introduced in [5, 6]. In [7], a printed rectangular ring monopole antenna with symmetrical L-strips is presented. A rectangle-loaded monopole antenna with inverted-L slot is reported in [8]. A printed inverted-L shaped monopole antenna with parasitic inverted-F element for dual-band applications is proposed in [9]. The latter antenna covers only the 2.4/5.2/5.8 GHz WLAN applications. In addition, a CPW fed printed monopole antenna with branch slits for WiMAX applications has been studied in [10] which covers only the WiMAX bands (2.5–2.7, 3.3–3.8 and 5.2–5.8 GHz). A monopole antenna with hybrid strips and a CPW-fed planar monopole antenna with three patch strips have been proposed in [11, 12]. However, these two latter proposed antennas can not cover the 2.6/5.5 GHz WiMAX bands and the 5.2 GHz WLAN band. A broadband antenna employing simplified metamaterial transmission lines (SMTLs) is proposed in [13], and this antenna does not cover the 5.5 GHz WiMAX band and the 5.2/5.8 GHz WLAN bands. A printed monopole antenna using three branch strips and a monopole antenna with a pair of F-shaped stubs and a rectangular monopole radiator for 3.5/5.5 GHz WiMAX bands and 2.4/5.2/5.8 GHz WLAN bands are reported in [14, 15]. The designs of the planar antennas in [1-8, 16-26] have a large physical size and a complex geome-

try thus degrading their availabilities for practical applications. A simple multi-band planar monopole antenna with a small form is desirable to realize the required operating frequency bands for all WLAN/WiMAX operations.

In this paper, we propose a rectangular ring monopole antenna with a vertical strip which satisfies the WLAN standards (2.4–2.484 GHz/ 5.15–5.35 GHz/ 5.725–5.825 GHz) and WiMAX standards (2.5–2.69 GHz/ 3.4–3.69 GHz/ 5.25–5.85 GHz). The rectangular ring structure fulfills the 2.6/5.5 GHz and 2.4/5.2/5.8 GHz applications. By adding one straight strip to the inner edge of this rectangular ring without altering the size, a middle resonance frequency at 3.5 GHz WiMAX band is created. The proposed antenna provides two impedance bandwidths of 650 MHz and 2460 MHz for the working bands of 2.30-2.95 GHz and 3.40-5.86 GHz, respectively. Therefore, the suggested planar monopole antenna is well designed to achieve multi-band characteristics with sufficiently large bandwidths to cover the entire WLAN/WiMAX wireless communication applications. A prototype of this antenna is fabricated and tested. The simulated and measured results are presented and are found to be in a good agreement. Details of the antenna design and the parameters which affect the performance of the proposed antenna in terms of its frequency domain characteristics are studied and discussed.

The next parts of this article are organized as follows: Section 2 discusses the geometric details of the proposed antenna. Section 3 presents the parametric study of the proposed antenna. Section 4 provides proofs that the proposed antenna is well suited for multi-band WLAN/WiMAX wireless applications with its simulated and measured results. Finally, a conclusion is drawn.

2. ANTENNA STRUCTURE AND DESIGN

Coplanar waveguide (CPW) fed antennas have received much attention because of their wide operating bandwidth, low profile, low cost, simple fabrication, potential for integration with Monolithic Microwave Integrated Circuits (MMIC) and simple configuration using a single metallic layer [27]. A conventional CPW on a dielectric substrate consists of a center strip conductor with a pair of ground planes on either side separated by a small gap G, as shown in Fig. 1a.

Fig. 1b shows the geometry of the CPW-fed dual-band planar monopole antenna. The proposed antenna is implemented on a low-cost FR4 epoxy substrate which has a relative permittivity of $\varepsilon_r = 4.2$, a loss tangent of 0.016, a thickness of $h = 1.6$ mm, a total area of 19 (W) × 36 (L) mm^2 and a coppering thickness of the radiator $t = 0.035$ mm.

The proposed antenna is fed by a 50 Ω impedance CPW that has a central strip having as width W_f and the gap distance between the central feed line and the coplanar ground plane is G. The length of the rectangular ring monopole antenna is L_1 with a uniform width W_2. Furthermore, the dimension of the horizontal strip

line of this ring is W_1. The distance between the rectangular ring and the ground plane is L_2, the size of the vertical strip is $W_3 \times L_3$ and both ground planes with similar dimensions of $W_g \times L_g$ were placed on each side of the CPW line. To investigate the performance of the proposed antenna configuration in terms of achieving multi-band operations, a commercially available simulation software of CST Microwave Studio based on Finite Integration Technique (FIT) was used for the required numerical analysis and to obtain the appropriate geometrical parameters which are presented in Table 1.

Fig. 2 depicts the two stages of the proposed antenna design. Two diverse antennas are defined as Antenna (a) and Antenna (b). Fig. 3 presents the comparison of the simulated reflection coefficient (S_{11}) with respect to frequency for only the case with rectangular ring monopole (Antenna a) and the proposed antenna (Antenna b).

Table 1 – The optimal dimensions of the proposed antenna (Unit: mm)

Parameters	Dimensions (mm)
W	19
L	36
W_1	6.35
L_1	19
W_2	2.6
L_2	3.4
W_3	1.1
L_3	11.7
W_g	7.7
L_g	11.4
W_f	2.8
G	0.4

Antenna (a) in Fig. 2 is solely a rectangular ring monopole. This simple design can easily achieve two fundamental resonant modes at about 2.70 GHz and 5.60 GHz as shown in Fig. 3. It is seen from the result that the simulated impedance bandwidths for $S_{11} \leq -10$ dB are about 800 MHz (2.40-3.20 GHz) and 1000 MHz (5.10-6.10 GHz) for the lower and upper bands, respectively. The basic antenna structure (Antenna a) does not require any supplementary structures for dual-band 2.6/5.5 GHz and 2.4/5.2/5.8 GHz applications compared to the planar monopole antennas reported in [7, 15]. The latter antennas with a modified T-shaped stub [7] or a pair of F-shaped stubs [15] for dual-band WLAN characteristics have complex structures which limit their practical applications. Then, when the vertical strip is integrated in the inner edge of the rectangular ring monopole (Antenna b shown in Fig. 2), the lower resonant mode is decreased to be at about 2.66 GHz and the middle resonant frequency of 3.52 GHz is excited with an improvement in the impedance matching at 5.60 GHz (5-GHz band). For the proposed antenna, the simulated impedance bandwidths for $S_{11} \leq -10$ dB are about 570 MHz (2.40-2.97 GHz) and 2870 MHz (3.40-6.27 GHz) for the first and second bands, respectively as depicted in Fig. 3.
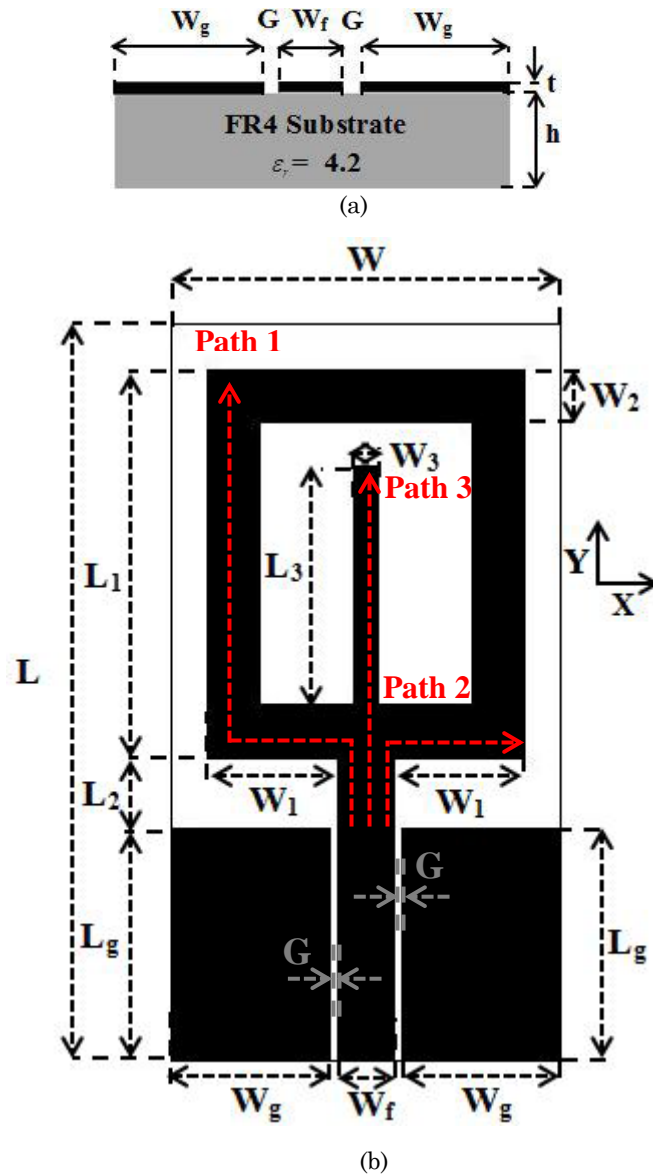
(a)

(b)

Fig. 1 – Geometry of the proposed antenna: (a) side view, (b) top view
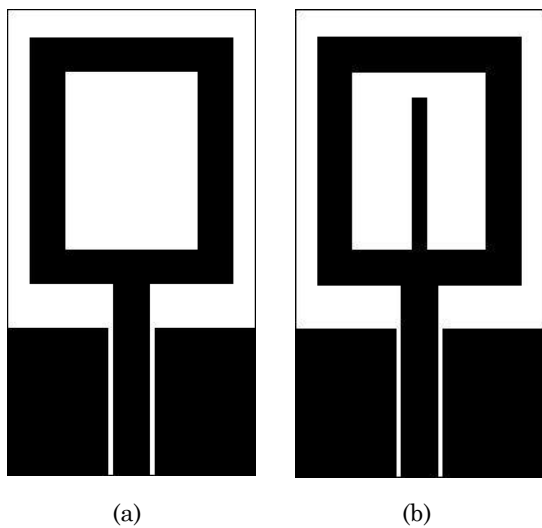

(a)　　　　　　(b)

Fig. 2 – Design stages of the proposed antenna: (a) basic antenna structure (Antenna a), (b) proposed antenna (Antenna b)
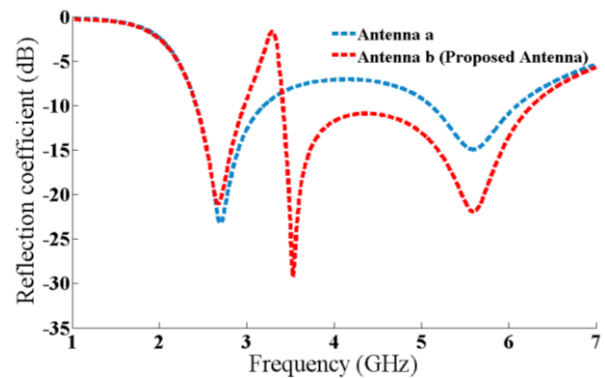

Fig. 3 – Reflection coefficient (S_{11}) with respect to frequency for the basic antenna structure (Antenna a) and the proposed antenna (Antenna b)

Clearly, the obtained bandwidths sufficiently cover the requirements of the 2.6/3.5/5.5 GHz WiMAX bands (2.5–2.69 GHz/ 3.4–3.69 GHz/ 5.25–5.85 GHz) and the 2.4/5.2/5.8 GHz WLAN bands (2.4–2.484 GHz/ 5.15–5.35

GHz/ 5.725–5.825 GHz). It is worthwhile noting that a good separation between the two operating frequency bands is obtained.

By applying a rectangular ring monopole antenna for lower and upper resonant modes (2.6/5.5-GHz and 2.4/5.2/5.8-GHz operations) and a vertical strip for middle resonant mode (3.5-GHz operation), it is found that the proposed antenna has much simpler configuration and smaller size for multi-band wireless communication applications. The bandwidths and the resonant frequencies for the basic antenna structure (Antenna a) and the proposed antenna (Antenna b) are listed in Table 2. It is important to mention that a good adaptation in the two operating bands is remarked.

Table 2 – Comparison between the basic antenna structure (Antenna a) and the proposed antenna (Antenna b)

	Antenna a	Antenna b
First band	2.40–3.20 GHz BW$_1$ = 800 MHz	2.40–2.97 GHz BW$_1$ = 570 MHz
Second band	5.10–6.10 GHz BW$_2$ = 1000 MHz	3.40–6.27 GHz BW$_2$ = 2870 MHz
Resonant frequencies/ Level reflection coefficient (S_{11})	f_{r1} = 2.70 GHz $S_{11}(f_{r1})$ = – 23 dB f_{r2} = 5.60 GHz $S_{11}(f_{r2})$ = – 15 dB	f_{r1} = 2.66 GHz $S_{11}(f_{r1})$ = – 21 dB f_{r2} = 3.52 GHz $S_{11}(f_{r2})$ = – 29 dB f_{r3} = 5.60 GHz $S_{11}(f_{r3})$ = – 22 dB

In the geometry, the resonant path length T_1 ($T_1 = L_2 + W_1 + L_1$), T_2 ($T_2 = L_2 + W_2 + L_3$), T_3 ($T_3 = L_2 + W_1$) of the rectangular ring monopole and vertical strip are set close to quarter-wavelength at their fundamental resonant frequencies, and could be calculated by the following equations:

$$T_1 = \frac{C}{4 f_{r_1} \sqrt{\varepsilon_{reff}}}, \qquad (2.1)$$

$$T_2 = \frac{C}{4 f_{r_2} \sqrt{\varepsilon_{reff}}}, \qquad (2.2)$$

$$T_3 = \frac{C}{4 f_{r_3} \sqrt{\varepsilon_{reff}}}, \qquad (2.3)$$

$$\varepsilon_{reff} = \frac{\varepsilon_r + 1}{2}, \qquad (2.4)$$

where C is the speed of light, ε_r is the relative permittivity of the substrate and ε_{reff} is the effective relative permittivity.

f_{r1} and f_{r3} denote the fundamental resonant frequencies of the rectangular ring monopole. In this study, f_{r1} and f_{r3} are selected to be 2.60 GHz and 5.60 GHz, respectively. The rectangular ring is employed to operate at both the lower and upper bands.

f_{r2} denotes the fundamental resonant frequency of the vertical strip. In this study, f_{r2} is selected to be 3.50 GHz and the vertical strip is adopted to create the

middle resonant frequency at 3.5-GHz WiMAX band.

The initial antenna design is provided by the design equations (2.1) to (2.4) without considering the mutual coupling between the rectangular ring monopole and the vertical strip. The accurate design of the proposed antenna needs to be adjusted and optimized using CST Microwave Studio simulator. The optimized dimensions of design parameters shown in Fig. 1 are introduced in Table 1. In the next step, a detailed parametric study is performed to investigate the effects of the key structure parameters on the antenna performances.

3. PARAMETRIC STUDY

In this proposed design, the first band (2.40–2.97 GHz) and the second band (3.40–6.27 GHz) are obained mainly because of the use of the rectangular ring monopole and the vertical strip. By changing the parameters L_1, W_1, L_2, L_3 and W_2, a parametric study is made to illustrate the influences of these dimensions on antenna reflection coefficient result. The study is based on the antenna structure shown in Fig. 1b.
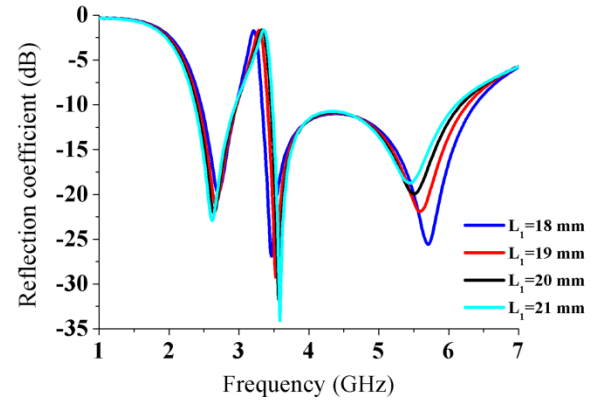
(a)
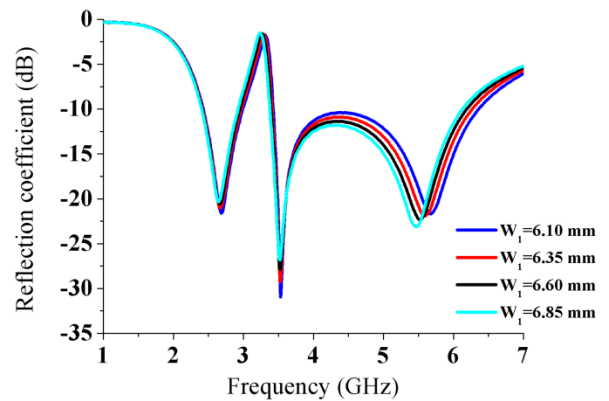
(b)

Fig. 4 – Reflection coefficient S_{11} for various values of (a) L_1 and (b) W_1

Fig. 4a shows the effects of varying the length of the rectangular ring L_1 on the reflection coefficient when the width of the antenna is fixed at $W_1 = 6.35$ mm, the distance between the rectangular ring and the ground plane is fixed at $L_2 = 3.4$ mm and the vertical strip with length $L_3 = 11.7$ mm. We notice that when we vary the parameter L_1 from 18 mm to 21 mm both the first and

third resonant modes shift towards a lower frequency, while the second resonant mode is slightly affected. The resonant frequencies at the lower and higher bands range from 2.70 GHz to 2.62 GHz and 5.71 GHz to 5.45 GHz, respectively.

Fig. 4b shows the variation of reflection coefficient with change in width W_1 of the rectangular ring while keeping all other dimensions unchangeable ($L_1 = 19$ mm, $L_2 = 3.4$ mm and $L_3 = 11.7$ mm). As W_1 increases from 6.10 mm to 6.85 mm with an interval of 0.25 mm, the reflection coefficient rises in the higher resonant mode with a shifting of the resonant frequency from 5.67 GHz to 5.47 GHz, whereas the lower and middle resonant frequencies keep almost unchanged. The width of the rectangular ring monopole has a major impact on the upper frequency band (5-GHz band). We notice that the properties of the upper frequency band can be efficiently controlled by adjusting the dimension W_1 of the horizontal strip line of the rectangular ring monopole antenna. Therefore, it can be concluded that the main function of the rectangular ring monopole is to create two resonant modes at the lower and upper frequency bands without additional structures to preserve the miniaturization of the proposed antenna for 2.6/5.5-GHz and 2.4/5.2/5.8-GHz wireless communication systems.

Fig. 5a presents the effect of changing the distance between the rectangular ring and the ground plane L_2 ($L_1 = 19$ mm, $W_1 = 6.35$ mm and $L_3 = 11.7$ mm) on the reflection coefficient of the proposed antenna. We remark that the variation of the parameter L_2 has an influence in controlling the 5 GHz band matching. The first band and the 3.5 GHz WiMAX band are shifted towards a lower frequency when L_2 is varied from 2.6 mm to 3.8 mm.

The effect of varying parameter W_2 on reflection coefficient of the proposed antenna is illustrated in Fig. 5b. When the dimension of W_2 increases from 1.6 mm to 3.1 mm with a step of 0.5 mm, the lower and upper resonant modes were shifted to a higher frequency. Further, the bandwidth of the second band broadens from 2.5 GHz (3.44–5.94 GHz) to 3 GHz (3.36–6.36 GHz) with a good impedance matching ($S_{11} = -22$ dB at 5.60 GHz) when the width W_2 is selected to be 2.6 mm. On the other hand, the middle resonant frequency is slightly affected. Our obtained result indicates that the impedance bandwidth of the second band can be effectively controlled by adjusting the dimension of the uniform width of the rectangular ring monopole antenna. The parameter W_2 plays a key role to enhance the bandwidth of the second band, which is wide enough to cover the WiMAX 3.5/5.5-GHz and WLAN 5.2/5.8-GHz applications.

Fig. 5c displays the simulation of the reflection coefficient against frequency for various values of L_3 ($L_1 = 19$ mm, $W_1 = 6.35$ mm and $L_2 = 3.4$ mm). By changing the length of L_3 from 10.7 mm to 12.2 mm, it is clear that the raise in L_3 decreases the middle resonant frequency (L_3 has a significant effect on the 3.5-GHz resonant mode). On the other hand, the first band and the 5 GHz band (upper resonant frequency) remain unaltered. The 3.5 GHz WiMAX band can be

controlled in an efficient manner by tuning the dimension L_3 of the vertical strip.
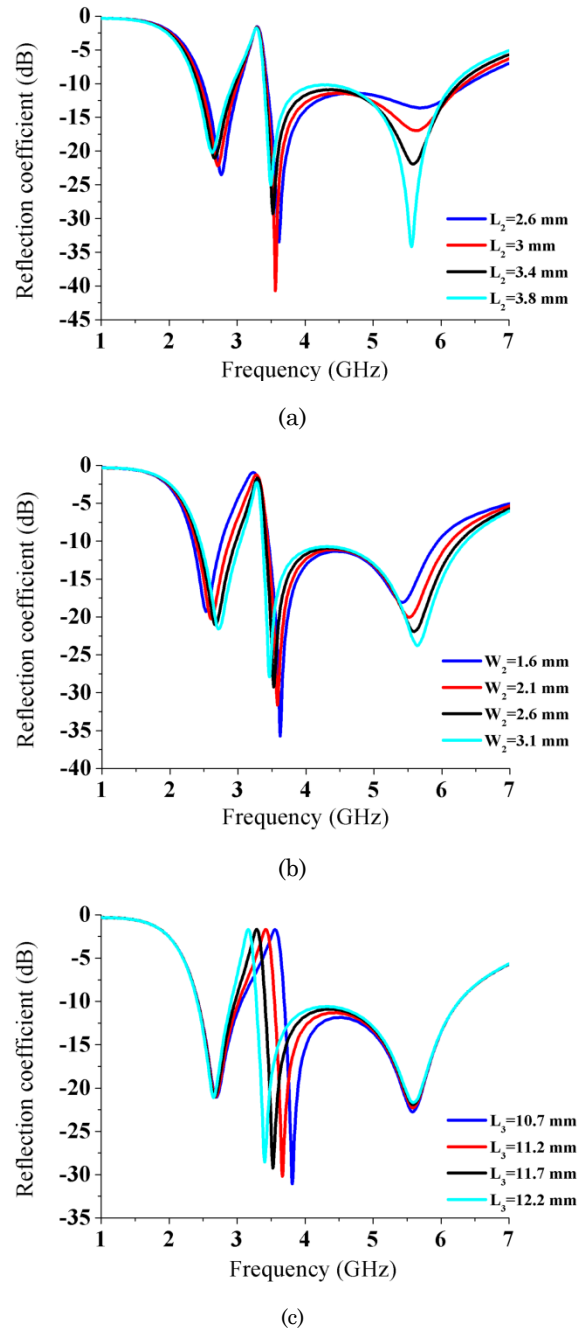

(a)

(b)

(c)

Fig. 5 – Reflection coefficient S_{11} for various values of (a) L_2, (b) W_2 and (c) L_3

## 4. RESULTS AND DISCUSSION

4.1 Reflection Coefficient Results

The dual-band planar monopole antenna is simulated using both CST Microwave Studio and HFSS. A prototype structure of the proposed antenna has been constructed and experimentally studied. The final design was made on a substrate FR4 epoxy with a permittivity of $\varepsilon_r = 4.2$, a thickness of $h = 1.6$ mm, a loss tangent of 0.016 and a 35 μm of metallization thickness. The SMA female connector is used for feeding with characteristic

impedance of 50 Ω. The reflection coefficient is measured with Hewlett-Packard HP 8720D vector network analyzer, which has a frequency range limited to 20 GHz. Fig. 6 shows the simulated and measured results of the reflection coefficient of the proposed antenna with the optimized parameters. The measured impedance bandwidths for $S_{11} \leq -10$ dB are about 650 MHz (2.30–2.95 GHz, $f_{r1} = 2.60$ GHz) and 2460 MHz (3.40–5.86 GHz, $f_{r2} = 3.61$ GHz and $f_{r3} = 5.21$ GHz), which makes it easy to cover the required bandwidths for WiMAX standards (2.5–2.69 GHz/ 3.4–3.69 GHz/ 5.25–5.85 GHz) and WLAN standards (2.4–2.484 GHz/ 5.15–5.35 GHz/ 5.725–5.825 GHz). For the proposed design, we note a good agreement between the simulated and measured results with a good impedance matching in the desired operating bands confirming its potential for multi-band wireless communication systems.
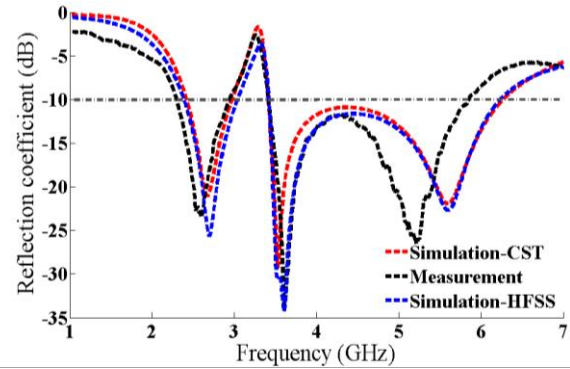
Fig. 6 – Measured and simulated results of the reflection coefficient (S_{11}) with respect to frequency for the proposed antenna

(a)   (b)   (c)   (d)
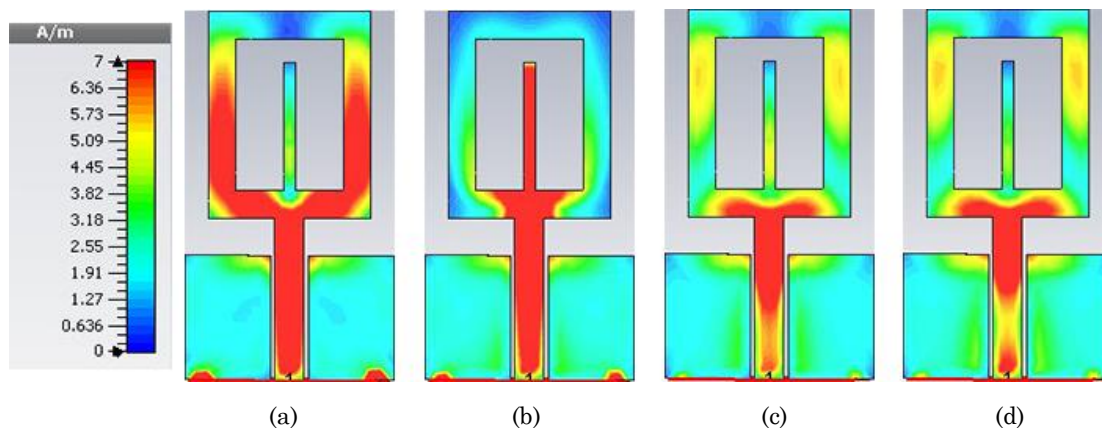
Fig. 7 – Simulated surface current distributions of the proposed antenna at (a) 2.60 GHz, (b) 3.50 GHz, (c) 5.20 GHz and (d) 5.50 GHz

4.2 Current Distributions Results

In order to further demonstrate the dual-band operation mechanism, the surface current distributions on the whole proposed antenna at different resonant frequencies are shown in Figs. 7a-d. It can be evidently seen that the current has different distributions along the optimized structure in different bands. Fig. 7a shows that the current distributions are forced to flow around the vertical strip line of the rectangular ring. The current distributions at frequency 2.60 GHz is found to be similar to resonant Path 1, as shown in Fig. 1b. Figs. 7c and 7d depict the current distributions at frequencies 5.20 GHz and 5.50 GHz. The horizontal strip line of the rectangular ring contributed essentially to radiation at frequencies of 5.20 GHz and 5.50 GHz. The resonant currents at frequencies of 5.20 GHz and 5.50 GHz are distributed on the horizontal strip line which is similar to resonant Path 2, as shown in Fig. 1b. Thus, both the lower and upper bands (2.6/5.5-GHz and 2.4/5.2/5.8-GHz applications) can be achieved by suitably adjusting the lengths of both the vertical and horizontal strip lines of the rectangular ring monopole antenna. As perceived in Fig. 7b, the current distributions at 3.50 GHz are mainly around the vertical strip used on the inner edge of the rectangular ring. The middle band for WiMAX 3.5 GHz application is thus obtained by tuning the length of the vertical strip. The resonant currents at frequency 3.50 GHz are distributed on the

vertical strip which is similar to resonant Path 3, as shown in Fig. 1b.

Table 3 compares the measured and simulated results of the impedance bandwidths for the proposed antenna. We notice that there is a sufficient bandwidth at the two bands to cover the entire WLAN and WiMAX bands.

4.3 Radiation Patterns, Gain and Efficiency of the Antenna

Fig. 8 and Fig. 9 show the simulated and measured radiation patterns in H-plane (XZ plane) and E-plane (YZ plane) for the frequencies of 2.40 GHz, 2.60 GHz, 3.50 GHz, 5.20 GHz and 5.50 GHz, respectively.

These results reveal that fairly good omnidirectional patterns are achieved in the H-plane over the operating bands, and the patterns in the E-plane are almost bidirectional. A very good agreement between measurements and simulations is also noted.

Fig. 10 shows the simulated gain and radiation efficiency versus the frequency of the proposed antenna. For the first band, the antenna gain varies from 1.4 to 2.08 dBi and the radiation efficiency varies between 67 % and 84.9 %. Then, in the second band, the gain and radiation efficiency variations are from 1.08 to 5.1 dBi and from 67.5 % to 89.9 %.

A comparative study of the proposed antenna with other planar antennas in terms of size, total occupied

Table 3 – A comparison between measured and simulated impedance bandwidths of the proposed antenna

|	CST Simulation	HFSS Simulation	Measurement
First band	2.40–2.97 GHz (BW_1 = 570 MHz / 21%)	2.39–3.04 GHz (BW_1 = 650 MHz / 24%)	2.30–2.95 GHz (BW_1 = 650 MHz / 25%)
Second band	3.40–6.27 GHz (BW_2 = 2870 MHz / 51%)	3.40–6.24 GHz (BW_2 = 2840 MHz / 50%)	3.40–5.86 GHz (BW_2 = 2460 MHz / 47%)
Resonant frequencies	f_{r1} = 2.66 GHz f_{r2} = 3.52 GHz f_{r3} = 5.60 GHz	f_{r1} = 2.70 GHz f_{r2} = 3.60 GHz f_{r3} = 5.60 GHz	f_{r1} = 2.60 GHz f_{r2} = 3.61 GHz f_{r3} = 5.21 GHz

(a)

(b)

(c)

(d)

(e)
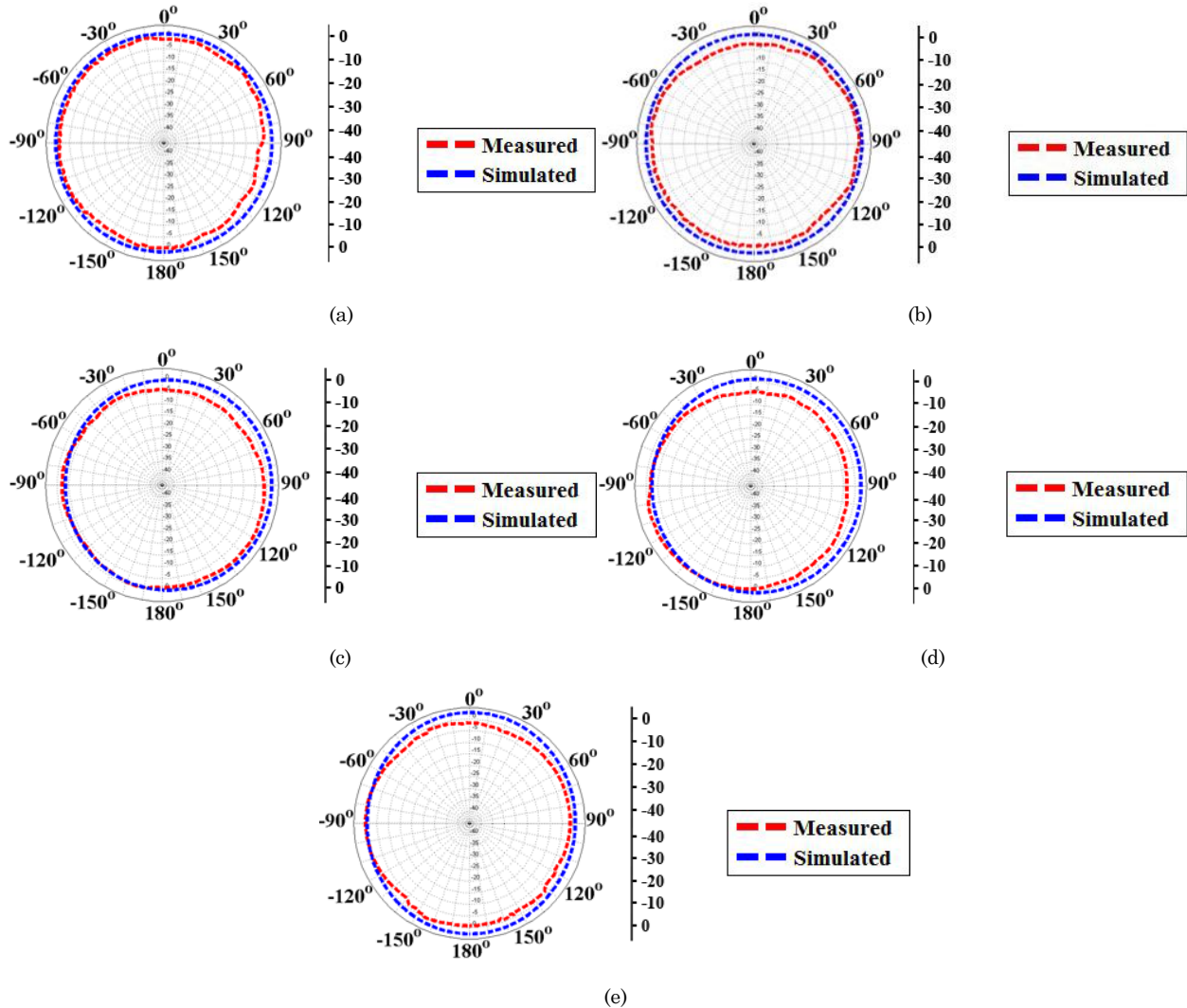
Fig. 8 – Comparison between simulated and measured radiation patterns in H-plane for the proposed antenna at frequencies (a) 2.40 GHz, (b) 2.60 GHz, (c) 3.50 GHz, (d) 5.20 GHz and (e) 5.50 GHz

area and the frequency of operation has been summarized in Table 4. From this comparative study table, it is evident that the proposed multi-band antenna occupies the smallest area knowing that it has a simpler geometry compared to other mentioned designs with a sufficient bandwidth at both the desired operating bands to cover the entire WLAN and WiMAX wireless applications.

5. CONCLUSION

A miniaturized CPW-fed planar monopole antenna with multi-band characteristics has been investigated in this article. The proposed antenna consists of a rectangular ring as well as a vertical strip with the main function of creating the middle resonant frequency at 3.50 GHz. The antenna has a small size of 19×36 mm^2 and a simple structure. The effects of varying dimensions of key structure parameters on the antenna performance are studied. The monopole antenna was designed, fabricated and tested. There is close agreement between the measurement and simulation results. The measured -10 dB reflection coefficient bandwidths range from 2.30 to 2.95 GHz (650 MHz) and from 3.40 to 5.86 GHz (2460 MHz) for the first and second bands, respectively covering both the 2.4/5.2/5.8 GHz WLAN and 2.6/3.5/5.5 GHz WiMAX standards. Moreover, the proposed antenna has several advantages, such as

(a)

(b)

(c)

(d)

(e)
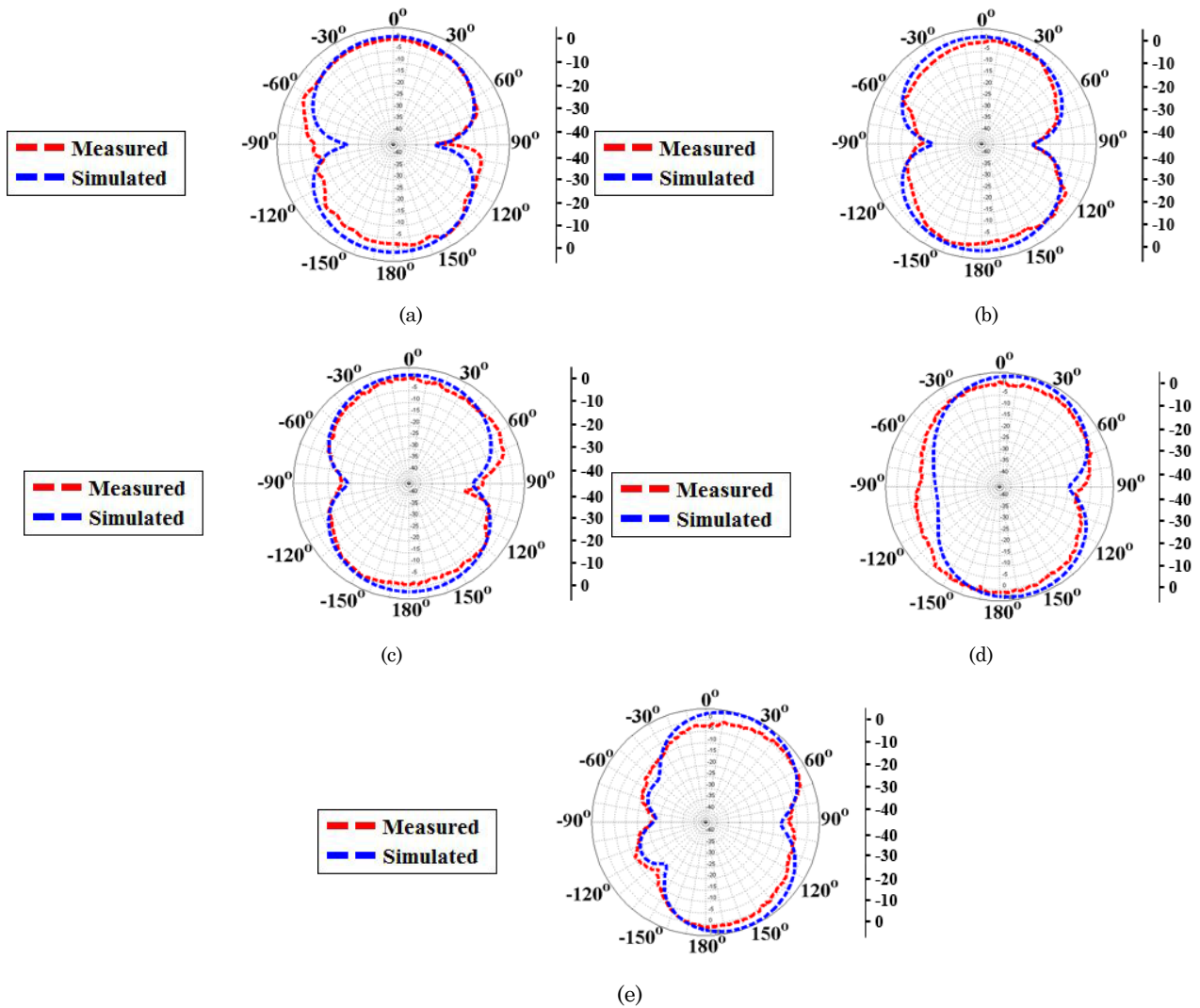
Fig. 9 – Comparison between simulated and measured radiation patterns in E-plane for the proposed antenna at frequencies (a) 2.40 GHz, (b) 2.60 GHz, (c) 3.50 GHz, (d) 5.20 GHz and (e) 5.50 GHz

Table 4 – Performance comparison of the proposed antenna with other reported multi-band antennas

Reference number	Antenna size (mm × mm)	Total area occupied (mm²)	Frequency of operation (GHz)
[1]	30 × 35	1050	2.4/2.5/3.5 5.2/5.5/5.8
[2]	27.1 × 38.8	1051.48	2.4/2.5/3.5 5.2/5.5/5.8
[4]	28 × 32	896	2.4/2.5/3.5 5.2
[9]	40 × 30	1200	2.4/5.2/5.8
[10]	35 × 45	1575	2.5/3.5/5.5
[11]	20 × 38	760	2.4/3.5/5.8
[12]	20 × 40	800	2.4/3.5/5.8
[14]	17.5 × 40	700	2.45/3.6/5.2 5.8
[15]	23 × 36	828	2.4/3.5/5.2 5.5/5.8
[18]	50 × 30	1500	2.45/5.2/5.8
[19]	23 × 36.5	839.5	2.4/2.5/3.5 5.8
[20]	64 × 62	3968	2.4/3.5/5.8
[22]	25 × 30	750	2.6/3.5/5.5
[24]	30 × 36	1080	2.5/3.5/5.6
[25]	22.6 × 32	723.20	3.5/5.2/5.5 5.8
Proposed antenna	19 × 36	684	2.4/2.6/3.5 5.2/5.5/5.8
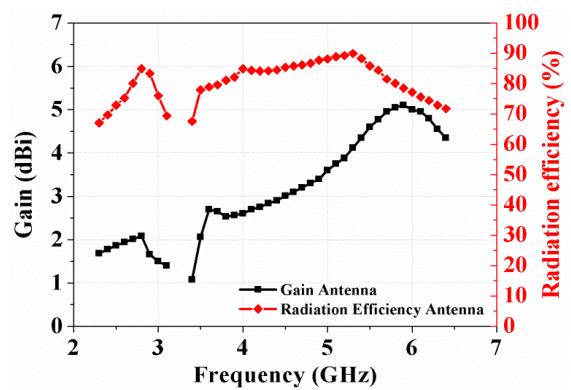
Fig. 10 – Simulated gain and radiation efficiency with respect to frequency for the proposed antenna

excellent radiation patterns and higher gains, which makes it a good candidate for WLAN/WiMAX wireless communication applications.

REFERENCES

1. L. Dang, Z.Y. Lei, Y.J. Xie, G.L. Ning, J. Fan, *IEEE Antennas Wireless Propag. Lett.* **9**, 1178 (2010).
2. S. Jo, H. Choi, J. Lim, B. Shin, S. Oh, J. Lee, *Int. J. Antennas Propag.* **2015**, 165270 (2015).
3. A. Kunwar, A.K. Gautam, B.K. Kanaujia, *Int. J. Microw. Wirel. Technol.* **9** No 1, 191 (2017).
4. W. Hu, Y.-Z. Yin, P. Fei, X. Yang, *IEEE Antennas Wireless Propag. Lett.* **10**, 462 (2011).
5. H. Zhai, Z. Ma, Y. Han, C. Liang, *IEEE Antennas Wireless Propag. Lett.* **12**, 65 (2013).
6. J. Pei, A.-G. Wang, S. Gao, W. Leng, *IEEE Antennas Wireless Propag. Lett.* **10**, 298 (2011).
7. X. Li, W. Hu, Y.F. Wang, X.W. Shi, X.T. Gu, *Microw. Opt. Technol. Lett.* **54** No 4, 1049 (2012).
8. H. Chen, X. Yang, Y.-Z. Yin, J.-J. Wu, Y.-M. Cai, *Electron. Lett.* **49** No 20, 1261 (2013).
9. S. Verma, P. Kumar, *Microw. Opt. Technol. Lett.* **56** No 5, 1163 (2014).
10. W.-S. Chen, Y.-C. Chang, *Microw. Opt. Technol. Lett.* **50** No 4, 952 (2008).
11. X. Ren, S. Gao, Y. Yin, *Microw. Opt. Technol. Lett.* **57** No 1, 94 (2015).
12. H.U. Iddi, M.R. Kamarudin, T.A. Rahman, A.Y. Abdulrahman, M. Khalily, M.F. Jamlos, *Microw. Opt. Technol. Lett.* **55** No 9, 2209 (2013).
13. C. Zhou, G. Wang, J. Liang, Y. Wang, B. Zong, *IEEE Antennas Wireless Propag. Lett.* **13**, 595 (2014).
14. C.-H. Ku, L.-K. Li, W.-L. Mao, *Microw. Opt. Technol. Lett.* **52** No 8, 1858 (2010).
15. Z. Tang, K. Liu, Y. Yin, R. Lian, *Microw. Opt. Technol. Lett.* **57** No 10, 2298 (2015).
16. Y. Xu, Y.-C. Jiao, Y.-C. Luan, *Electron. Lett.* **48** No 24, 1519 (2012).
17. Y. Li, W. Yu, *Int. J. Antennas Propag.* **2015**, 146780 (2015).
18. C.-Y. Huang, E.-Z. Yu, *IEEE Antennas Wireless Propag. Lett.* **10**, 500 (2011).
19. P. Liu, Y. Zou, B. Xie, X. Liu, B. Sun, *IEEE Antennas Wireless Propag. Lett.* **11**, 1242 (2012).
20. L. Peng, C.-L. Ruan, X.-H. Wu, *IEEE Antennas Wireless Propag. Lett.* **9**, 1069 (2010).
21. C.-M. Peng, I.-F. Chen, J.-W. Yeh, *IEEE Antennas Wireless Propag. Lett.* **12**, 898 (2013).
22. J.-H. Lu, B.-J. Huang, *Electron. Lett.* **46** No 10, 671 (2010).
23. C. Wang, P. Xu, B. Li, Z.-H. Yan, *Microw. Opt. Technol. Lett.* **53** No 9, 2016 (2011).
24. X.Q. Zhang, Y.C. Jiao, W.H. Wang, *Electron. Lett.* **48** No 2, 64 (2012).
25. S. Chen, M. Fang, D. Dong, M. Han, G. Liu, *Microw. Opt. Technol. Lett.* **57** No 8, 1769 (2015).
26. W.-C. Liu, C.-M. Wu, Y. Dai, *IEEE T. Antennas Propag.* **59** No 7, 2457 (2011).
27. H.D. Chen, H.T. Chen, *IEEE T. Antennas Propag.* **52** No 4, 978 (2004).